

# Thermoviscoelastic Modeling Approach for Predicting the Recovery Behaviors of Thermally Activated Amorphous Shape Memory Polymers

GU Jianping<sup>1,3\*</sup>, FANG Changqing<sup>2,3</sup>, SUN Huiyu<sup>3</sup>, ZHANG Xiaopeng<sup>1</sup>

1. Jiangsu Key Laboratory of Advanced Structural Materials and Application Technology, School of Materials Science and Engineering, Nanjing Institute of Technology, Nanjing 211167, P. R. China;

2. Shanghai Space Propulsion Technology Research Institute, Shanghai 201109, P. R. China;

3. State Key Laboratory of Mechanics and Control of Mechanical Structures, Nanjing University of Aeronautics and Astronautics, Nanjing 210016, P. R. China

(Received 06 May 2018; revised 19 November 2018; accepted 06 January 2019)

**Abstract:** A thermoviscoelastic modeling approach is developed to predict the recovery behaviors of the thermally activated amorphous shape memory polymers (SMPs) based on the generalized finite deformation viscoelasticity theory. In this paper, a series of moduli and relaxation times of the generalized Maxwell model is estimated from the stress relaxation master curve by using the nonlinear regression (NLREG) method. Assuming that the amorphous SMPs are approximately incompressible isotropic elastomers in the rubbery state, the hyperelastic response of the materials is well modeled with a hyperelastic model in Ogden form. In addition, the Williams-Landel-Ferry (WLF) equation is used to describe the horizontal shift factor obtained with time-temperature superposition principle (TTSP). The finite element simulations show good agreement with the experimental thermomechanical behaviors. Moreover, the possibility of developing a temperature-responsive intravascular stent with the SMP studied here is investigated in terms of its thermomechanical property. Therefore, it can be concluded that the model has good prediction capabilities for the recovery behaviors of amorphous SMPs.

**Key words:** shape memory polymers (SMPs); thermoviscoelastic modeling approach; finite deformation; recovery behavior

**CLC number:** TB381

**Document code:** A

**Article ID:** 1005-1120(2019)05-0798-10

## 0 Introduction

Shape memory polymers (SMPs) have drawn considerable attention in recent years for their capability to recover a large pre-deformed shape under an environmental stimulus such as temperature, light, humidity, solution, electric field or magnetic field<sup>[1-5]</sup>. SMPs have plenty of advantages over shape memory alloys (SMAs), such as low cost, light weight, electrical insulation, excellent manufacturability, adjustable transition temperature, potential biocompatibility and biodegradability. Besides, a maximum strain of 200% can be stored by SMPs<sup>[6]</sup>,

compared with that of only about 8% by SMAs<sup>[7]</sup>. Therefore, SMPs have broad applications in many fields including clothing manufacturing, sensor and actuators, self-deployable structures in spacecraft, morphing aircraft and intelligent medical devices<sup>[8-11]</sup>.

Though being outstanding in many aspects compared with SMAs, SMPs still have shortcomings of much lower recovery stress, much longer recovery time and shorter cycle life, etc<sup>[12]</sup>. Obviously, the mechanical performance of SMPs can be improved by reinforcing fillers. Therefore, a great variety of shape memory polymer composites (SMPCs)

\*Corresponding author, E-mail: gujianping@njit.edu.cn.

**How to cite this article:** GU Jianping, FANG Changqing, SUN Huiyu, et al. Thermoviscoelastic Modeling Approach for Predicting the Recovery Behaviors of Thermally Activated Amorphous Shape Memory Polymers[J]. Transactions of Nanjing University of Aeronautics and Astronautics, 2019, 36(5):798-807.

<http://dx.doi.org/10.16356/j.1005-1120.2019.05.011>

have been developed recently. Apart from the reinforcement effect, new stimulus methods, novel shape memory effects (SMEs) and rich applications can be enabled or enhanced by many SMPCs.

In general, the achievements made in constructing effective mechanical models for SMPs and SMPCs are much less than that made in developing novel SMPs and SMPCs. The thermally activated amorphous SMPs have great potential in many aspects for their relative simple trigger mechanism. Therefore, the main purpose of this paper is to develop a new modeling approach to predicting the recovery behaviors of these materials. The following discussion is under the condition that the glass transition mechanism accounts for the SMEs of the thermally activated amorphous SMPs.

So far, the modeling approaches for amorphous SMPs have been classified into two categories, i.e., phase transition modeling and thermoviscoelastic modeling<sup>[13]</sup>. In order to describe the shape storage and recovery effects, the first phase transition model in which the material was divided into frozen and active phases was proposed by Liu et al. in 2006<sup>[14]</sup>. Thereafter, Qi et al. and Baghani et al. further developed the phase transition modeling approaches<sup>[15-16]</sup>. It should be noticed that the phase transition approaches describe a nonphysical process which does not occur in real SMPs and this should be the major shortcoming of these approaches. Though the phase transition modeling approaches are commonly used in modeling crystallizable polymers, their phenomenological representations provide useful predictive tools<sup>[17-19]</sup>. The first three-dimensional (3D) finite deformation thermoviscoelastic model which is an extension of the three elements standard linear rheological solid was proposed by Diani et al.<sup>[20]</sup> Nguyen et al.<sup>[21]</sup> further developed the model by using the theory of structural and stress relaxation to account for the underlying shape memory mechanisms. Xiao et al.<sup>[22-23]</sup> improved the model incorporated with multiple discrete structural and stress relaxation processes and enabled it to describe the viscoplastic yielding and flow behavior of the glassy material at low temperatures. Although these thermoviscoelastic models

can well describe and predict the thermomechanical behaviors of SMPs, they are complicated and a large number of material parameters should be determined, which limit their application. To tackle the problem, Diani et al.<sup>[24]</sup> used a commercial finite element code to predict the torsion shape storage and recovery behaviors of the SMP in large-deformation small-strain condition, by assuming that the thermomechanical property solely depends on the material viscoelasticity coupled with its time-temperature superposition property (TTSP). In the model, the generalized Maxwell model and Williams-Landel-Ferry (WLF) equation were used to describe the viscoelastic behavior and the TTSP, respectively. Besides, the neo-Hookean model is used to describe the hyperelastic response of the material in large-deformation condition. It should be noted that the modeling approach is convenient since it only needs an easy and standard use of the code<sup>[25]</sup>. Arrieta et al.<sup>[26]</sup> extended the model to large-strain uniaxial tension by using the similar approach. It is found that the model can predict both free length strain recovery and constrained length stress recovery well. In order to predict the free recovery behavior of the SMPs, Ge et al.<sup>[27]</sup> presented a simple one-dimensional model containing only eight parameters based on a modified standard linear solid model incorporating Kohlrausch-Williams-Watts stretched relaxation. In fact, the thermomechanical behaviors and the SMEs of the same material in the same experimental conditions were also predicted by Westbrook et al.<sup>[28]</sup>, by using a 3D finite deformation constitutive model incorporated with a multi-branch modeling approach for nonequilibrium relaxation processes. Unlike the modeling approaches presented by Ge et al.<sup>[27]</sup> and Westbrook et al.<sup>[28]</sup>, this study presents a thermoviscoelastic modeling approach in the framework of the approach developed by Diani et al.<sup>[24]</sup> to predict the recovery behaviors of the amorphous SMPs in uniaxial compression. The relevant experimental conditions and results can be found in Refs. [27-28].

In the work of Diani et al.<sup>[24]</sup> and Arrieta et al.<sup>[26]</sup>, a set of dynamic mechanical analysis (DMA) tests were conducted to obtain the values of storage modulus as a function of frequency at different tempera-

tures. By applying the TTSP, the values of the storage modulus as a function of frequency can be obtained for an otherwise unmeasurable wide range of frequencies. Then the parameters of the generalized Maxwell model were determined by fitting this storage modulus master curve. Herein, an alternative approach for the determination of the parameters of the generalized Maxwell model will be adopted, which is based on the test of stress relaxation. As demonstrated previously, the Ogden model can provide the best fitting to the stress-strain behavior of the SMPs at high temperatures, among various strain energy<sup>[29]</sup>. Therefore, it is used in this paper instead of the Neo-Hookean model.

Moreover, the possibility of developing a temperature-responsive stent using the material synthesized by Ge et al.<sup>[27]</sup> and Westbrook et al.<sup>[28]</sup> is investigated in the thermomechanical aspect.

## 1 Modeling and Implementation

The main purpose of this paper is to develop a modeling approach to predicting the recovery behaviors of the amorphous SMPs. The material used here is synthesized following Ref.[30]. Briefly, the tert-butyl acrylate (tBA) monomer and crosslinker poly-(ethylene glycol) dimethacrylate (PEGDMA) were mixed according to a pre-calculated ratio, and 2,2-dimethoxy-2-phenylacetophenone was added as the photoinitiator<sup>[27]</sup>. To determine the thermomechanical property and SME of the material, the relevant tests were performed by Ge et al.<sup>[27]</sup> and Westbrook et al.<sup>[28]</sup> Therefore, the corresponding experimental conditions and results can be found in Refs. [27-28].

### 1.1 Model description

Similar to the models presented by Ref. [24, 26], the generalized Maxwell model together with the TTSP are used to describe the thermoviscoelastic behaviors of the amorphous SMPs. In Ref. [24, 26], the parameters of the generalized Maxwell model were determined from the storage modulus master curve, i.e. the curve of the storage modulus values as a function of frequency, by using the method of nonlinear regularization (NLREG). In

Ref.[27], the experiments of stress relaxation at 13 different temperatures were carried out. Therefore, a relaxation master curve at 27.5 °C can be constructed by shifting individual relaxation curves with shifting factors at different temperatures, based on the TTSP. The experimental data can be found in Ref. [27]. Therefore, the parameters of the generalized Maxwell model are obtained from the stress relaxation master curve in this paper. Specifically, the relaxation Young modulus can be first expressed as

$$E(t) = E_{\infty} + E_i \exp\left(\frac{-t}{\tau_i}\right) \quad (1)$$

where  $E_{\infty}$  is the relaxation Young modulus at time  $t = \infty$ ,  $E_i$  and  $\tau_i$  are the relaxation Young modulus and relaxation time of the  $i$ th branch at the reference temperature. In this paper, the reference temperature is 27.5 °C and  $E_{\infty}$  is set to be 3 MPa which is slightly lower than the smallest value of the stress relaxation master curve. Whereafter, 30 pairs of relaxation Young moduli and relaxation times are determined from the stress relaxation master curve by using an NLREG program of a commercial mathematics software Matlab named LSQNONLIN, which are listed in Table 1.

Fig.1 shows the comparison between the stress relaxation master curve identified by using the generalized Maxwell model and obtained from the experiment. Obviously, the simulation results show good agreement with the experimental data.

For simplicity, only the WLF equation is used to describe the horizontal shift factor  $a_T$  obtained by using the TTSP.

$$\log a_T = \frac{-C_1(T - T_r)}{C_2 + T - T_r} \quad (2)$$

where  $C_1$  and  $C_2$  are the material constants, and  $T_r$  is the reference temperature. The values of  $C_1$ ,  $C_2$  and  $T_r$  are 17.44, 51.6 and 27.5 °C, respectively, which are equal to that of Ref. [27]. Additionally, the storage Young moduli  $E'(\omega)$ , loss Young moduli  $E''(\omega)$  and  $\tan \delta$  can be derived from the following equations

$$E'(\omega) = E_c + \sum_{i=1}^n E_i \frac{\omega^2 \tau_i^2}{1 + \omega^2 \tau_i^2} \quad (3a)$$

$$E''(\omega) = \sum_{i=1}^n E_i \frac{\omega \tau_i}{1 + \omega^2 \tau_i^2} \quad (3b)$$

**Table 1 Relaxation Young moduli and relaxation times of the generalized Maxwell model**

Parameter	Value					
$E_1-E_6$ / MPa	$2.22 \times 10^{-14}$	$1.90 \times 10^{-6}$	$7.47 \times 10^{-2}$	$1.08 \times 10^{-1}$	$1.29 \times 10^{-1}$	$6.33 \times 10^{-1}$
$\tau_1-\tau_6$ / s	$9.98 \times 10^5$	$1.0 \times 10^7$	$1.0 \times 10^7$	$1.0 \times 10^8$	$1.0 \times 10^9$	$9.68 \times 10^5$
$E_7-E_{12}$ / MPa	3.11	5.94	8.61	8.61	9.02	9.02
$\tau_7-\tau_{12}$ / s	$8.56 \times 10^4$	$1.27 \times 10^4$	$2.05 \times 10^{-6}$	$2.22 \times 10^{-14}$	$2.22 \times 10^{-14}$	$2.27 \times 10^{-6}$
$E_{13}-E_{18}$ / MPa	9.02	9.73	$1.24 \times 10^1$	$1.94 \times 10^1$	$1.94 \times 10^1$	$2.52 \times 10^1$
$\tau_{13}-\tau_{18}$ / s	$4.17 \times 10^{-6}$	$2.22 \times 10^{-14}$	$2.98 \times 10^3$	$8.56 \times 10^2$	$8.56 \times 10^2$	$8.53 \times 10^2$
$E_{19}-E_{24}$ / MPa	$8.90 \times 10^1$	$9.10 \times 10^1$	$9.10 \times 10^1$	$9.33 \times 10^1$	$9.34 \times 10^1$	$9.83 \times 10^1$
$\tau_{19}-\tau_{24}$ / s	$1.63 \times 10^1$	$5.81 \times 10^{-7}$	$1.09 \times 10^{-5}$	5.68	$1.64 \times 10^1$	5.68
$E_{25}-E_{30}$ / MPa	$1.23 \times 10^2$	$1.24 \times 10^2$	$1.40 \times 10^2$	$1.47 \times 10^2$	$1.49 \times 10^2$	$2.82 \times 10^2$
$\tau_{25}-\tau_{30}$ / s	$1.86 \times 10^2$	$1.86 \times 10^2$	$1.58 \times 10^{-1}$	2.02	$8.75 \times 10^{-1}$	$4.43 \times 10^1$

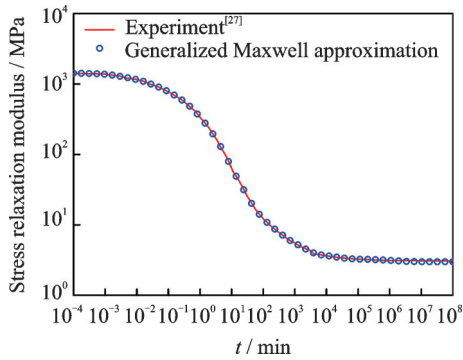


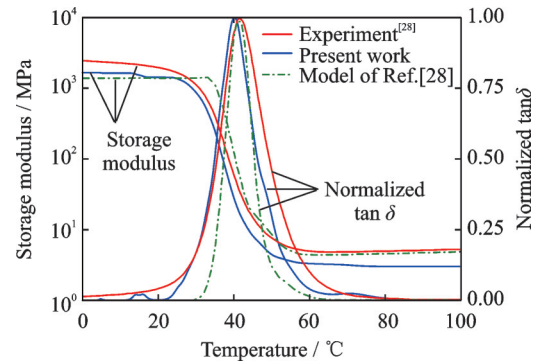
Fig.1 Comparison between the stress relaxation master curve predicted by the model and the experiment

$$\tan \delta = \frac{E''(\omega)}{E'(\omega)} \quad (3c)$$

where  $\omega$  is the frequency. Then the temperature-dependent storage modulus and the relative  $\tan \delta$  which is normalized to the maximum can be derived from Eq. (3) together with the WLF equation at a constant frequency. In Ref.[28], the DMA data of the SMP were obtained from a temperature sweep test at 1 °C/min, 0.2% strain and 1 Hz, as shown in Fig. 2<sup>[28]</sup>. The comparison between the simulation results and experimental data for the temperature-dependent storage modulus and the normalized  $\tan \delta$  is shown in Fig. 2. Clearly, the simulation results of present work fit well with the existing experimental data, which validates the fitting process in this paper. Here, the results predicted by Ref.[28] are also illustrated in Fig.2. Generally, the predictability of this paper is a little better than that of Ref.[28] in this aspect.

The coefficients of thermal expansion (CTE) for this material can be found in Ref. [28] (see Fig. 2). It should be noted that the CTE values

change a little from 0 °C to 100 °C at a rate of 1 °C/min. Since the CTE values for the material in the glassy state and rubbery state are  $1.25 \times 10^{-4}/^{\circ}\text{C}$  and  $2.52 \times 10^{-4}/^{\circ}\text{C}$ , respectively, an intermediate value of  $2.0 \times 10^{-4}/^{\circ}\text{C}$  is used here for simplicity. Though the CTE value is not precise, it may have little influence on the thermomechanical response of the material since the value is relatively small.

Fig.2 Comparison between the simulation and the experiment for the temperature dependent storage modulus and normalized  $\tan \delta$ 

The proposed model is simple without any adjustable parameters. Moreover, the model parameters are not obtained by fitting the shape memory thermomechanical experiments but on the routine tests for material property. Therefore, the advantage of this modeling approach is that the model is convenient to construct and the parameters could be easily determined. While it is worth noting that the model is relatively simple as compared with the real behavior of the material, since the effect of heat conduction and the response of pressure on the relaxation are not considered.

## 1.2 Finite element simulation

As a commercial software for finite element calculation, Abaqus has been proved to be successful in estimating the nonlinear mechanical behaviors of the materials. Since both the generalized Maxwell model and the WLF equation are available in Abaqus, the model is implemented in this software. The generalized Maxwell model is based on the linear viscoelasticity theory which is only used to account for the small strain viscoelasticity behavior. While the extension of the generalized Maxwell model for finite strain and large deformation is also available in Abaqus, which only requires a reference elastic model for finite strain and large deformation without modifying the relaxation times and relaxation moduli. Assuming that the amorphous SMPs are approximately incompressible isotropic elastomers in the rubbery state, a hyperelastic model is used as the reference elastic model. The hyperelastic material is described in terms of a "strain energy potential". In Ref. [28], isothermal uniaxial compression tests were performed at temperatures between 0 and 100 °C to explore the rubbery and glassy behavior<sup>[28]</sup>. For comparison, the strain energy potential in the forms of Ogden model, Mooney-Rivlin model and Neo-Hookean model are used to capture the material hyperelastic behavior at a high temperature, as shown in Fig. 3. The best fitting to the test can be obtained by the Ogden model. Therefore, the Ogden model will be used here, instead of the Neo-Hookean model used by Ref.[24, 26]. As shown in Fig. 3, the parameters of the hyperelastic model in

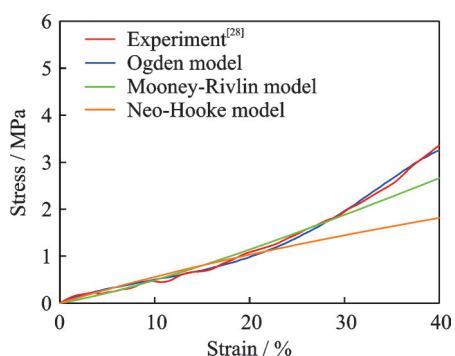


Fig.3 Comparison between the stress - strain response at 60 °C predicted by the hyperelastic models and the experiment

Ogden form can be determined in Abaqus by fitting the stress and strain relationship at the temperature well above the glass transition temperature  $T_g$  (40 °C). The parameters values are listed in Table 2.

**Table 2 Parameters of the hyperelastic model in Ogden form used in Abaqus**

$i$	$\mu_i$	$\alpha_i$
1	1 507 556.28	13.373 735 7
2	3 199 970.66	24.999 849 3
3	-1 731 166.32	-12.390 898 4

Since the VISCOELASTIC option of the Abaqus requires the shear relaxation modulus  $G_i$  rather than the relaxation Young modulus  $E_i$  provided by the generalized Maxwell model, the relaxation Young modulus  $E_i$  should be converted to the shear relaxation modulus  $G_i$  by assuming that the bulk modulus  $K$  is 1 130 MPa and temperature-independent<sup>[26]</sup>. The cylindrical deformable part of the specimen (both the diameter and the height are 10 mm) for compression is meshed with eight-node biquadratic axisymmetric quadrilateral hybrid element (CAX8H).

## 1.3 Results

The detailed experimental conditions for the shape memory cycle in Ref. [28] are presented as follows. For these experiments, the cylindrical SMP specimen was initially allowed to equilibrate at the programming temperature. During an shape memory cycle experiment, both free and constrained conditions during the recovery step were explored. The thermomechanical test temperatures for the free and constrained recovery are listed in Table 3. At the loading temperature, a compressive strain of 20% was applied to the specimen at a rate of 0.01 s<sup>-1</sup>. Then the specimen was allowed to relax for 10 min before cooled to the lowest temperature (shape fixing temperature) which is used to fix the temporary shape at a rate of 2.5 °C/min. Once the temperature reached the shape fixing one, the specimen was held for 60 min. After experiencing these programming steps, the specimen could deform freely without any constraint as the temperature increased at a rate of 2.5 °C /min in the

free recovery test. Once the temperature reached the required value, some time was given to the specimen to stabilize. In contrast with the free re-

covery test, the length of the specimen was fixed in the constrained recovery test. Here, the total time for the both recovery processes was 60 min.

**Table 3 Thermomechanical test temperature condition for the free and constrained recovery**

Description	Loading	Cooling	Recovery
Free recovery/°C	40	20	30, 35, 40 and 50
Constrained recovery/°C	60	10	60

The finite element simulations incorporated with the model developed here are run under the same conditions as those of temperature and deformation used experimentally. Fig.4 shows the simulation results of the stress of programming for both the free and constrained recoveries as a function of time. Clearly, the compressive stress of the loading at 40 °C is much higher than that at 60 °C since the relaxation time of the material at the lower temperature is longer. The compressive stress decreases fast in the cooling step. Once the compressive stress vanishes, the temporary shape is obtained. Fig.5 shows the comparison between the finite element predictions and the experiments for free recovery. Generally, the model could well predict the free recovery process of the material except that the onset of the strain recovery of the simulation is a little earlier than that of the experiment. Fig.6 shows the recovered stresses of the constrained recovery experiment and the model. It is clear that there are some discrepancies between the results of model prediction and experiment. The peak stress of the simulation is lower than that of the test. Besides, the onset of the stress recovery of the simulation is shifted to a higher temperature. However, it should be noted that the general stress evolution of the model is consis-

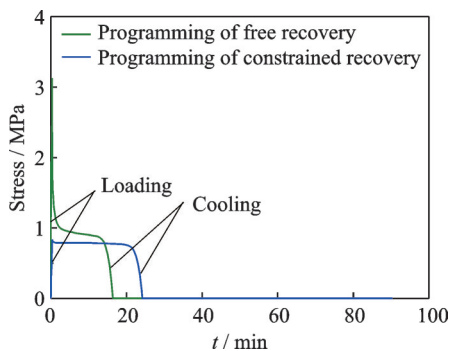


Fig.4 Stress as a function of programming time

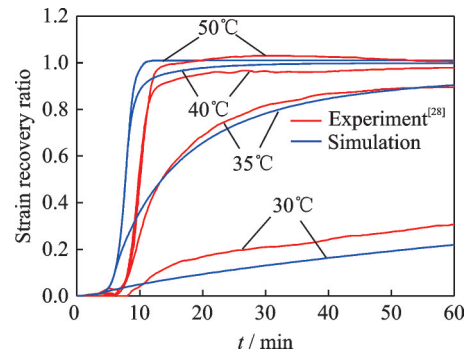


Fig.5 Comparison between the simulation and the experiment for free recovery

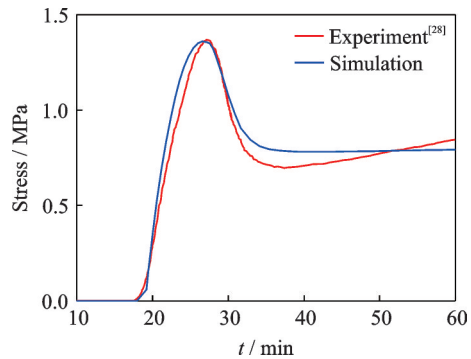


Fig.6 Comparison between the simulation and the experiment for constrained recovery

tent with that of the test, and the final recovery stress of the simulation is close to that of the test.

In general, the model used in this paper could well predict the recovery behaviors of the amorphous SMP. Since  $T_g$  of the material studied in this paper is near the normal body temperature of the human, i. e., 37 °C, the possibility of developing a temperature-responsive medical stent with this material will be investigated in terms of the thermo-mechanical aspect in the following section.

## 2 Medical SMP Stent

A realistic stent made of the amorphous SMP

can be implanted into the blood vessel. In Fig.7, the stent has an inner radius of  $R_i = 10$  mm and an outer radius of  $R_o = 12$  mm. The diameter of the uniformly distributed holes is 2 mm. Since the SMEs of the stent are concerned primarily, only a quarter of the periodic part of the stent geometry is analyzed due to the symmetry, as shown in Fig.8.



Fig.7 Geometry and finite element discretization of a medical stent

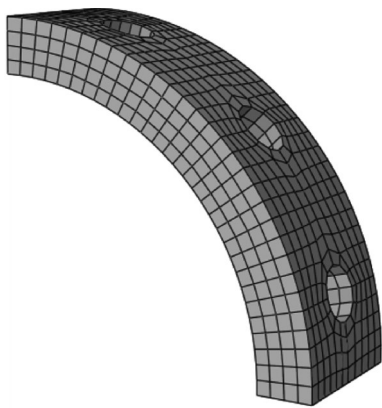


Fig.8 Geometry and finite element discretization of a quarter of the periodic part of the stent

Here the simulation is carried out for a typical four-step thermomechanical history:

**Step 1** The pressure that increases linearly from 0 to 0.13 MPa within 10 s is applied to the top and the bottom surfaces of the stent at 40 °C.

**Step 2** The shape is fixed by the external constraint and then the temperature decreases at a rate of 2.5 °C/min.

**Step 3** Once it reaches 20 °C, the external constraint is removed and the temporary shape is obtained.

**Step 4** The stent is heated to the human body temperature (37 °C) when it is implanted into the blood vessel. For simplicity, the heating rate is assumed to be 2.5 °C/min. Once it reaches 37 °C, some time is given to the specimen to stabilize. The

total time for this step is 30 min.

The contours in Fig.9 refer to the deformation and the von-Mises stress of the periodic part at different steps of the thermomechanical cycle. The initial state and the post-pressed state are shown in Figs.9(a, b). Fig. 9(c) shows the temporary shape of the stent. The stent in this state can be implanted into the blood vessel and then heated to the body temperature. In Fig. 9(d), the original shape is recovered perfectly, which represents that the stent can hold the blood vessel open to a certain degree.

### 3 Conclusions

Based on the generalized finite deformation viscoelasticity theory, a thermoviscoelastic modeling approach is presented to predict the recovery behaviors of the thermally activated amorphous SMPs. In contrast to the earlier approaches developed by Ref. [24, 26], a series of moduli and relaxation times of the generalized Maxwell model is estimated from the stress relaxation master curve rather than the storage modulus master curve, by using the NLREG method. The horizontal shift factor is described by the WLF equation. The simulation results of present work fit well with the existing experimental data for the temperature-dependent storage modulus and normalized  $\tan\delta$  of the material, which validates the fitting approach in this paper. Since the extension of the generalized Maxwell model for finite strain and large deformation is available in Abaqus, which only requires a reference elastic model, a hyperelastic model in Ogden form is used here to model the hyperelastic response of the material.

Generally, comparisons between the simulation results and the recovery experiments show an acceptable agreement. Therefore, the model has good prediction capabilities for the recovery behaviors of the amorphous SMPs. Moreover, the possibility of developing a temperature-responsive stent with the material studied in this paper is investigated in the thermomechanical aspect. The simulation results show that the stent can hold the blood vessel open to a certain degree after experiencing a typical

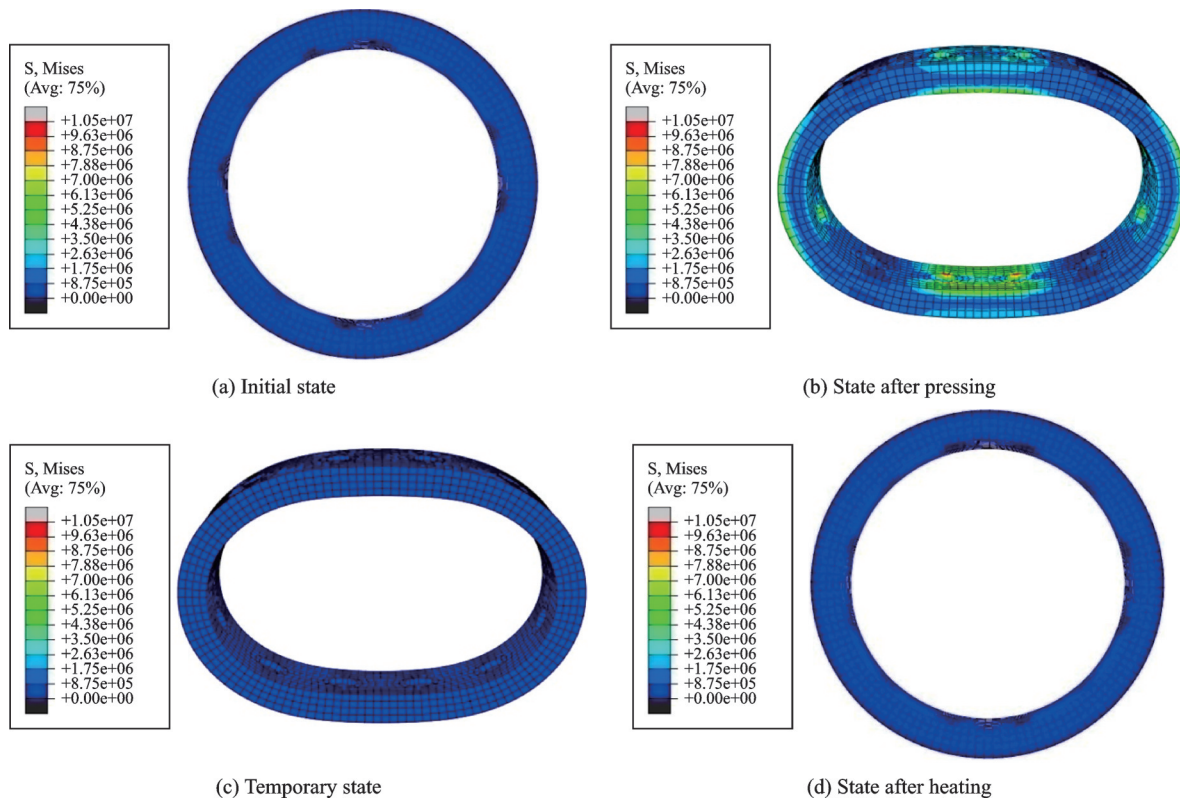


Fig.9 Deformation and stress for a typical thermomechanical cycle

thermomechanical history.

It should be noted that the advantage of the proposed modeling approach is that the model is convenient to construct and the parameters could be easily determined from the routine tests for material property. The shortcoming is that the model is relatively simple as compared with the real behavior of the material, thus resulting in some quantitative differences between the model predictions and experiments. Therefore, an accurate model with more predictive capabilities should be further developed in the future.

**References**

[1] LI G, WANG A. Cold, warm, and hot programming of shape memory polymers[J]. *Journal of Polymer Science Part B-Polymer Physics*, 2016, 54(14): 1319-1339.

[2] LU H B, DU S Y. A phenomenological thermodynamic model for the chemo-responsive shape memory effect in polymers based on Flory-Huggins solution theory[J]. *Polymer Chemistry*, 2014, 5(4): 1155-1162.

[3] XIAO R. Modeling solvent-activated shape-memory behaviors based on an analogy between solvent and temperature[J]. *RSC Advances*, 2016, 6(8): 6378-6383.

[4] LENG J S, LYU H B, LIU Y J, et al. Electroactive shape-memory polymer filled with nanocarbon particles and short carbon fibers[J]. *Applied Physics Letters*, 2007, 91(14): 144105.

[5] HARDY J G, PALMA M, WIND S J, et al. Responsive biomaterials: Advances in materials based on shape-memory polymers[J]. *Advanced Materials*, 2016, 28(27): 5717-5724.

[6] LIU Y J, LYU H B, LAN X, et al. Review of electro-active shape-memory polymer composite[J]. *Composites Science and Technology*, 2009, 69(13): 2064-2068.

[7] LIU B F, WANG Q F, HU S L, et al. Thermodynamic behaviors of functionally graded shape memory alloy actuator[J]. *Journal of Nanjing University of Aeronautics and Astronautics*, 2017, 49(S): 45-50. (in Chinese)

[8] LENG J S, LAN X, LIU Y J, et al. Shape-memory polymers and their composites: Stimulus methods and applications[J]. *Progress in Materials Science*, 2011, 56(7): 1077-1135.

[9] HU J, ZHU Y, HUANG H, et al. Recent advances in shape-memory polymers: Structure, mechanism, functionality, modeling and applications[J]. *Progress in Polymer Science*, 2012, 37(12): 1720-1763.

[10] ZHAO Q, Qi H J, XIE T. Recent progress in shape

- memory polymer: New behavior, enabling materials, and mechanistic understanding[J]. *Progress in Polymer Science*, 2015(49/50): 79-120.
- [11] HAGER M D, BODE S, WEBER C, et al. Shape memory polymers: Past, present and future developments[J]. *Progress in Polymer Science*, 2015 (49/50): 3-33.
- [12] PRETSCH T. Review on the functional determinants and durability of shape memory polymers[J]. *Polymers*, 2010, 2(3): 120-158.
- [13] NGUYEN T D. Modeling shape-memory behavior of polymers[J]. *Polymer Reviews*, 2013, 53(1): 130-152.
- [14] LIU Y P, GALL K, DUNN M L, et al. Thermomechanics of shape memory polymers: Uniaxial experiments and constitutive modeling [J]. *International Journal of Plasticity*, 2006, 22(2): 279-313.
- [15] QI H J, NGUYEN T D, CASTRO F, et al. Finite deformation thermo-mechanical behavior of thermally induced shape memory polymers[J]. *Journal of the Mechanics and Physics of Solids*, 2008, 56(5): 1730-1751.
- [16] BAGHANI M, NAGHDABADI R, ARGHAVANI J, et al. A thermodynamically-consistent 3D constitutive model for shape memory polymers[J]. *International Journal of Plasticity*, 2012, 35(35): 13-30.
- [17] LU H, YU K, HUANG W M, et al. On the Takayanagi principle for the shape memory effect and thermomechanical behaviors in polymers with multi-phases[J]. *Smart Materials and Structures*, 2016, 25(12): 125001.
- [18] BOATTIE, SCALET G, AURICCHIO F. A three-dimensional finite-strain phenomenological model for shape-memory polymers: Formulation, numerical simulations, and comparison with experimental data[J]. *International Journal of Plasticity*, 2016, 83: 153-177.
- [19] LI Y X, HE Y H, LIU Z S. A viscoelastic constitutive model for shape memory polymers based on multiplicative decompositions of the deformation gradient[J]. *International Journal of Plasticity*, 2017, 91: 300-317.
- [20] DIANI J, LIU Y P, GALL K. Finite strain 3D thermoviscoelastic constitutive model for shape memory polymers[J]. *Polymer Engineering and Science*, 2006, 46(4): 486-492.
- [21] NGUYEN T D, QI H J, CASTRO F, et al. A thermoviscoelastic model for amorphous shape memory polymers: Incorporating structural and stress relaxation[J]. *Journal of the Mechanics and Physics of Solids*, 2008, 56(9): 2792-2814.
- [22] XIAO R, CHOI J, LAKHERA N, et al. Modeling the glass transition of amorphous networks for shape-memory behavior [J]. *Journal of the Mechanics and Physics of Solids*, 2013, 61(7): 1612-1635.
- [23] NGUYEN T D, YAKACKI C M, BRAHMHATT P D, et al. Modeling the relaxation mechanisms of amorphous shapememory polymers[J]. *Advanced Materials*, 2010, 22(31): 3411-3423.
- [24] DIANI J, GILORMINI P, FREDY C, et al. Predicting thermal shape memory of crosslinked polymer networks from linear viscoelasticity[J]. *International Journal of Solids and Structures*, 2012, 49(5): 793-799.
- [25] YU L, ZHAN Y N, SHI Y F, et al. Numerical simulation for damping-controlled deployment of Z-folded inflatable tube[J]. *Transactions of Nanjing University of Aeronautics and Astronautics*, 2017, 34(4): 420-425.
- [26] ARRIETA S, DIANI J, GILORMINI P. Experimental characterization and thermoviscoelastic modeling of strain and stress recoveries of an amorphous polymer network[J]. *Mechanics of Materials*, 2014, 68(1): 95-103.
- [27] GE Q, YU K, DING Y F, et al. Prediction of temperature-dependent free recovery behaviors of amorphous shape memory polymers[J]. *Soft Matter*, 2012, 8(43): 11098.
- [28] WESTBROOK K K, KAO P H, CASTRO F, et al. A 3D finite deformation constitutive model for amorphous shape memory polymers: A multi-branch modeling approach for nonequilibrium relaxation processes[J]. *Mechanics of Materials*, 2011, 43(12): 853-869.
- [29] PULLA S S, SOURI M, KARACA H E, et al. Characterization and strain-energy-function-based modeling of the thermomechanical response of shape-memory polymers[J]. *Journal of Applied Polymer Science*, 2015, 132(18): 41861.
- [30] YAKACKI C M, SHANDAS R, LANNING C, et al. Unconstrained recovery characterization of shape-memory polymer networks for cardiovascular applications[J]. *Biomaterials*, 2007, 28(14): 2255-2263.

**Acknowledgements** This work is supported by the Natural Science Foundation of Jiangsu Province of China (No. BK20170759), the National Natural Science Foundation of China (No. 11572153), Jiangsu Government Scholarship for Overseas Studies, a project funded by the Priority Academic Program Development of Jiangsu Higher Education Institutions (PAPD), Outstanding Scientific and Technological In-

novation Team in Colleges and Universities of Jiangsu Province, and the Doctor Special Foundation and the Research Fund of Nanjing Institute of Technology (Nos. ZKJ201603, YKJ201312).

**Authors** Dr. **GU Jianping** received B.S. and Ph.D. degrees in Engineering Mechanics from Nanjing University of Science and Technology and Nanjing University of Aeronautics and Astronautics, in 2005 and 2016, respectively. He has published about 20 peer-reviewed journal papers. His doctoral dissertation was awarded as an excellent doctoral dissertation of Nanjing University of Aeronautics and Astronautics in 2017. At present, he is an associate professor of Engineering Mechanics at Nanjing Institute of Technology, China. He is the recipient of research grant from the Natural Science Foundation of Jiangsu Province of China (BK20170759). Dr. GU is engaged in the research of mechanical behaviors of shape memory polymers and their composites. His research interest includes thermomechanical modeling of smart materials and structures.

Dr. **FANG Changqing** received the B.S. and Ph.D. degrees in Engineering Mechanics from Nanjing University of Aeronautics and Astronautics, in 2011 and 2018, respectively. Dr. FANG is engaged in the research of mechanical behaviors of shape memory polymers and their composites. He has published about 10 peer-reviewed journal papers. In April 2018, he joined Shanghai Space Propulsion Technology Research Institute, as a researcher. His research interest includes modeling the shape memory behaviors of smart mate-

rials by using fractional order method.

Prof. **SUN Huiyu** received his Ph.D. degree from the University of California, Davis, USA, in 2005. Prof. SUN has conducted funded research on composite materials and smart materials for aerospace engineering. He has published about 50 peer-reviewed journal papers. Prof. SUN is the recipient of research grants from National Natural Science Foundation of China (11572153) and the Natural Science Foundation of Jiangsu Province of China (BK20151467). His research interest includes modeling the thermomechanical behaviors of smart materials and woven fabric composites.

Dr. **ZHANG Xiaopeng** received the B.S. degree in Engineering Mechanics in 2005 and Ph.D. degree in Material Science in 2013 from Harbin Institute of Technology, Harbin, China. In Aug. 2013, he joined the Department of Material Engineering, Nanjing Institute of Technology, Nanjing, China. His research interest includes dynamic mechanical behavior of lattice aluminum foam materials and low-temperature crystallization of alumina films.

**Author contributions** Prof. **SUN Huiyu** and Dr. **Gu Jianping** designed the study, Dr. **GU Jianping** developed the model, conducted the analysis and wrote the manuscript, Dr. **FANG Changqing** contributed data for the model analysis, and Dr. **ZHANG Xiaopeng** contributed to the background of the study.

**Competing interests** The authors declare no competing interests.

(Production Editor: Zhang Tong)